
# Special Course in signal analysis Report

**AUTHOR**

Chang Hui Simone Lin - s232963 - bjg199

September 26, 2024

# Contents

# 1 Introduction

## 1.1 Objective

The objective of this project is to analyze and correlate different kinds of data to look for a quantification of task conflict in a patient.

## 1.2 Movement

Movement can be thought of as the way our brain communicates with the physical world. In particular, voluntary movement allows humans to control the precise execution of various motor tasks with little effort. Walking is an example of a seemingly simple act but the underlying process consists of complex interactions between your brain, nerves, and muscles. Locomotor commands from higher supraspinal centers travel down to the brainstem and spinal cord, which initiate a coordinated sequence of muscle activations orchestrated by lower neural centers. However, this process is not solely top-down. Sensory feedback from muscles, joints, and other receptors continually modulates the movement[1], ensuring precise gait patterns and efficient locomotion. Thus, movement control relies on the coordinated actions of the brain and spinal cord, which also includes sensory feedback.

### 1.2.1 Brain Control of Movement

The central motor system is arranged as a hierarchy of control levels. Strategy regarding determining the objective of the movement and the most effective strategy to achieve it, is found at the highest level and is represented by the association areas of the neocortex and the basal ganglia in the forebrain. The middle level deals tactics by orchestrating the sequence of muscle contractions, coordinated in both space and time, essential for achieving the strategic objective as smoothly and accurately as possible. This is represented by the motor cortex and cerebellum. The lowest level, represented by the brain stem and spinal cord handles execution by initiating the activation of motor neuron and interneuron pools responsible for generating the goal-directed movement and making any required postural adjustments[2].

When it comes to controlling movement, the brain operates through two main pathways in the spinal cord. The first, known as the lateral pathways, is directly controlled by the cortex and is responsible for voluntary movements of the limbs, and helps control precise movement. Specifically, two of the lateral pathways namely the corticospinal and rubrospinal tracts, are crucial for motor control. The corticospinal tract originates from the neocortex and is the largest pathway in the central nervous system. It mainly carries commands from the frontal lobe to muscles on the opposite side of the body. Meanwhile, the rubrospinal tract, originating from the midbrain, also contributes to motor control, although its significance has decreased in humans over time. The second is the ventromedial pathways, which is managed by the brainstem, and is responsible of gross movements of proximal limbs and posture. The ventromedial pathways consist of four tracts originating in the brainstem. These tracts regulate spinal interneurons responsible for coordinating proximal and axial muscles, and they utilize

sensory input to reflexively maintain balance and posture. For instance, the vestibulospinal and tectospinal tracts manage head balance and orientation, while the reticulospinal tracts help regulate antigravity reflexes[2].

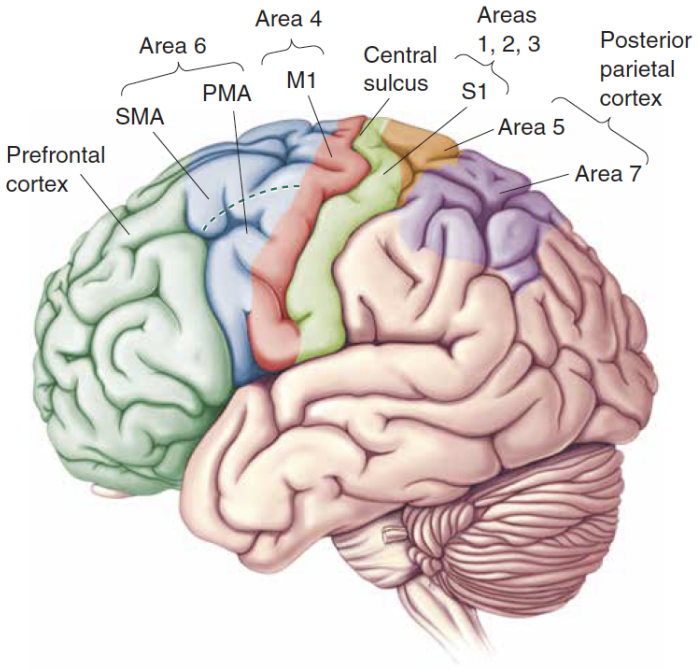


***Figure 1:*** *Areas of the neocortex that are involved in the planning and execution of voluntary movement. The motor cortex consists of areas 4 (M1) and 6 (PMA and SMA). Inputs are processed in the posterior parietal cortex. Taken from [2].*

Essential centers for planning and executing voluntary movements are found in neocortical motor areas, particularly areas 4 and 6 illustrated in Figure 1. Area 4, or the primary motor cortex (M1), initiates muscle contractions. Meanwhile, area 6, which includes the premotor area (PMA) and supplementary motor area (SMA), coordinates different muscle groups for skilled movement. To plan movements effectively, an internal body image is likely formed by inputs processed in the posterior parietal cortex, which collaborates with the frontal lobes in abstract thinking and decision-making. Axons from these regions converge on area 6, influencing movement intentions and planning. The ventral lateral nucleus of the thalamus plays a significant role, providing input to area 6 and influenced by the basal ganglia. This forms a loop regulating voluntary movement. The basal ganglia, composed of various nuclei, modulate motor functions through direct and indirect pathways, promoting selected actions and inhibiting others[2]. Pyramidal neurons in cortical layer V are crucial for activating lower motor neurons and coordinating muscle contractions. Other cortical areas and the thalamus are the two primary input sources to the layer V pyramidal cells in M1. Commanding the muscles to contract is oftentimes not enough. Many movements require a detailed sequence of muscle contractions, with varying amounts of generated force and timing. The cerebellum, plays a vital role in precise muscle coordination, particularly in the lateral cerebellum. It guides planned

movements by providing instructions to the motor cortex based on past experiences, contributing to motor learning and adjustments[2].

In summary, movement is a sophisticated interplay between the brain, nerves, and muscles, allowing for precise execution of motor tasks. Understanding the mechanisms behind movement control, both at the spinal and brain levels is crucial for understanding the complexities of locomotion. The spinal control of movement involves coordinated interaction between muscles, neurons, and sensory inputs, facilitating the generation of precise movements essential for tasks like walking. Meanwhile, the brain organizes movement through hierarchical pathways, with different levels of control ensuring effective planning, execution, and adjustment of movements. Key structures such as the motor cortex, basal ganglia, and cerebellum play vital roles in this process, enabling humans to perform various motor tasks with accuracy and synchronization.

## 1.3 Electromyography

Electromyography (EMG) is a technique for recording and analyzing the electrical activity produced by skeletal muscles. This method is widely used in both clinical and research settings to assess muscle health, function, and neuromuscular disorders. [2]

When a muscle contracts, action potentials are generated by muscle fibers. These signals are the result of electrical impulses from motor neurons. The sum of the action potentials from all active muscle fibers within the recording area creates a compound muscle action potential (CMAP), which can be detected by EMG. EMGs are usually surface or Intramuscular. Surface EMGs use electrodes placed on the skin over the muscle. This method is non-invasive and useful for measuring the activity of larger muscles. On the other hand, intramuscular EMGs involve inserting needle electrodes into the muscle. This method provides detailed information about the activity of individual muscle fibers and is more sensitive than sEMG.

A typical EMG system is made of electrodes to sense electrical changes, an amplifier to increase signal strength level, an Analog to Digital Converter (ADC) to quantify continuous data, and a data acquisition system to visualize and analyze EMG signals.

## 1.4 Task conflict

Cognitive control is defined as the set of abilities that allow for the effortful application and maintenance of goal-directed behaviors. Task conflict emerges when stimulus-driven behaviors are incongruent with current goals, necessitating the activation of a task control mechanism.[3]

An example where task conflict can be seen is the Stroop Task, where participants name the ink color of words while ignoring the word itself. This task creates conflict between the automatic reading behavior and the goal-directed task of color naming. Two types of conflict emerge from this task:

- Information conflict: occurs when the incongruent word and ink color lead to different

responses.

- Task conflict: occurs when the task demands (color naming) conflict with the automatic response (word reading).

Task control can be observed through reaction times (RTs). When task control fails, RTs in congruent trials slow down, leading to a reversed facilitation effect. Therefore, understanding task conflict can help in interpreting cognitive control mechanisms and in developing interventions for related pathological behaviors[3].

The conflict task approached in this study is explained as follows: the task consists of 200 trials that start with a visual stimulus of either a yellow circle or a blue triangle, followed by a vibration of either the index (D2) or the little finger (D5). Based on the visual stimuli and the vibration position, the response of the subject will be either homotopic (vibration and moving finger align) or heterotopic (vibration and moving finger not aligned). The subject is wearing an electrode on FDI (D2 abductor) and ADM (D5 abductor) as well as accelerometers on D2 and D5.

# 2 Methods

The project is divided into 3 main parts: EMG analysis, accelerometer analysis, and summary statistics of the results. Implementations are mostly in Matlab since the input data is Matlab-specific. An exception is made for the response box data since it had a different data structure that is easy to access with Python's libraries.

## 2.1 EMG analysis

The EMG dataset consists of 200 trials each with six channels. However, only the first two channels (1 is FDI and 2 is ADM) are used since the other ones are all noise. Each trial is triggered by a pulse that also triggers the vibration. Both vibration and user responses can be seen with different grades of clarity between different trials.

To start to work on the EMG file, some preliminary work needs to be done on the data. First of all, a band-pass filter at the $[40-400]Hz$ frequencies is applied to the raw EMG data to eliminate non-relevant information. A notch filter at $50Hz$ due to the powerline is not needed because the data has been already pre-processed. The lower limit of the filter is to eliminate motion artifacts [4]. The higher limit is defined by looking at the physiological maximal spike frequency [5]. Some physiological information is present outside of the considered bandwidth. However, it is not useful for this application. Afterward, the DC offset is removed by subtracting the signal mean from the EMG [6]. Moreover, the filter order is determined with the Fred-Harris rule:

$$N = \frac{f_s}{B} \cdot \frac{dB}{22} \tag{1}$$

With

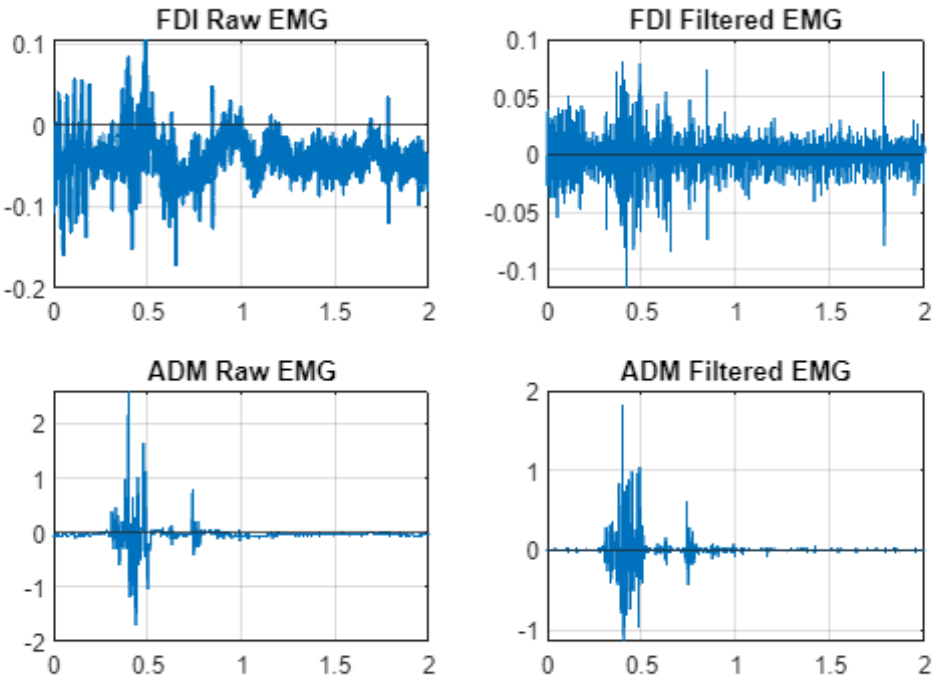


***Figure 2:*** *Plot Raw vs Filtered EMG.*

- $f_s$: sampling frequency
- $B$: bandwidth of interest
- $dB$: attenuation in $dB$

The results of these manipulations can be seen in Figure 2.

To further improve the readability of the data, rectification and enveloping are applied. Rectification is done by putting an absolute value on the signal, while enveloping is done by applying a low-pass filter with the cutoff frequency

$$f_c = \frac{1}{\Delta t} \tag{2}$$

With $\Delta t$ the time between the activation onset and the input box time. This value is in the order of $100ms$.

By applying the filter, it is possible to rest assured that the lift-off will be seen by the envelope. The criteria chosen to distinguish the signal from the background is

$$\text{EMG}_{envelope}(t) > 2\sigma \tag{3}$$

With $\sigma$ being the standard deviation. The results of the preliminary work can be seen in Figure 3

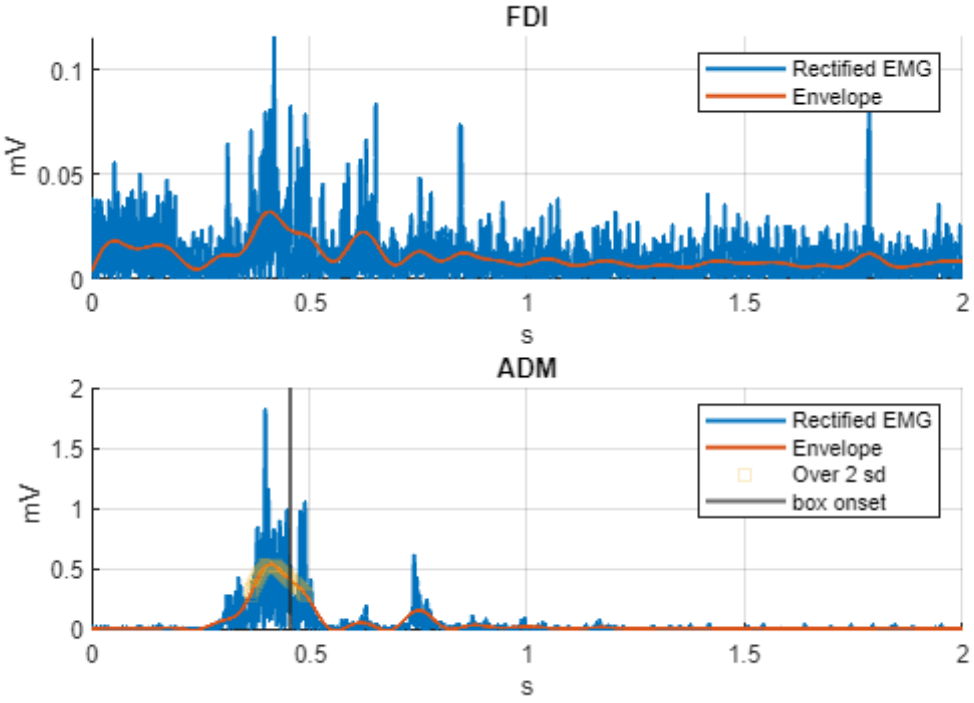


***Figure 3:*** *Plot of the rectified EMG signal with envelope. The onset time is the first instance where EMG$(t) > 2\sigma$, is earlier than the one registered by the box. This is physiologically reasonable since there is a delay between the signal, the movement, and the reaching of the target.*

Next, the power spectrum of the signal is calculated by applying a Fast Fourier Transformation (FFT) and calculating the power

$$P = \frac{|\text{EMG}(s)^2|}{n} \tag{4}$$

With

- EMG$(s)$: signal after the FFT
- $n$: number of samples

This can be used to determine if the responding finger is FDI or ADM as the responding finger will have higher power. The implementation considers the higher averaged power spectrum as the moving finger. The plot can be seen in Figure 4.

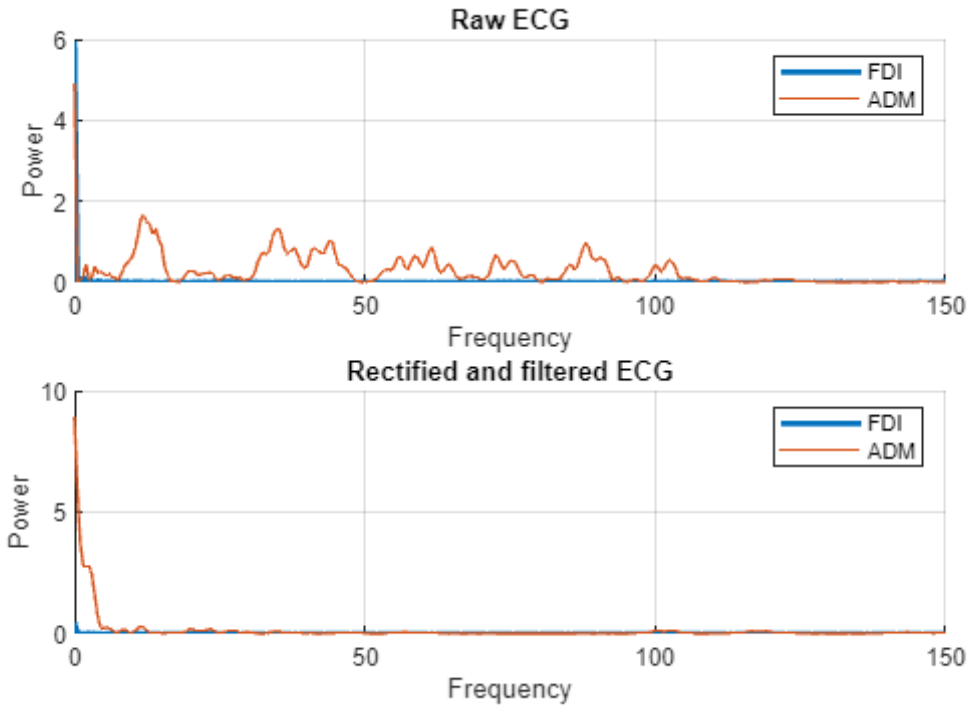


***Figure 4:*** *Plot of the power spectrum of the raw and filtered EMG data. Once the noise is filtered out, the power of the moving finger is much higher than the power of the resting finger.*

## 2.2 Accelerometer analysis

Accelerometer data is collected using a commercial device and a Magnetic Resonance (MR) compatible accelerometer. Each has three dimensions following the $x - y - z$ axis and is mounted on D2 and D5. However, in some cases, not all channels of the accelerometer work. The software triggers the device to record via a Python script corresponding to the one

discussed in Section 2.1. However, the segments are merged in one large data string, making it more challenging to approach.

Since accelerometer data is merged into one large data string, some preliminary filtering to isolate different kinds of information from the data is done. Specifically, filtering following the concepts of Section 2.1 is done. After calculating the power spectrum with Equation 4 and plotting it as shown in Figure 5, the vibration is isolated with a pass-band filter between $120 - 130Hz$ since it is less likely that a movement impacts those frequencies, while the movement is isolated with a pass-band filter between $1-10Hz$ since human movement energy is around those frequencies [7].

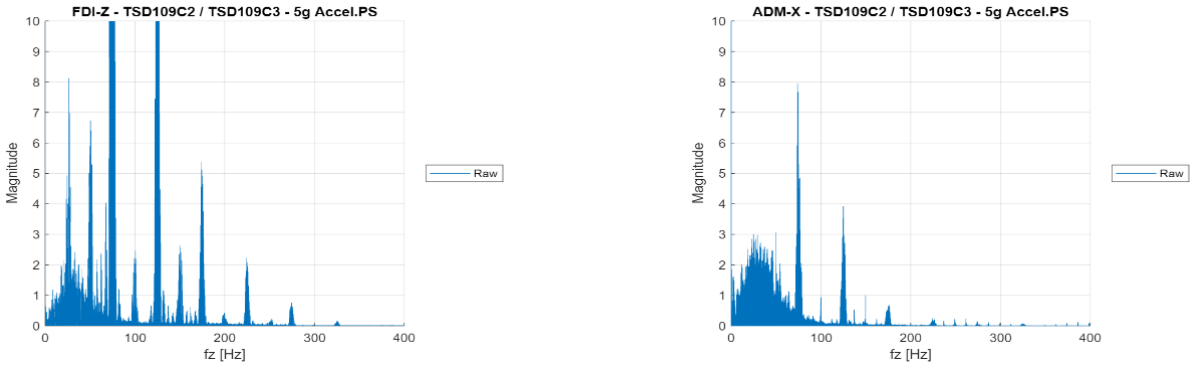


***Figure 5:*** *Power spectrum of accelerometer on D2 (left) and D5 (right). The $z$ channel for D2 has been chosen, while the $x$ channel for D5 has been chosen. The choice has been made on clarity of signal and sensitivity to movement and vibrations.*

Afterward, detection of the features is done by using the `find_peaks` function, and a lookout for the borders is done to get the onset and end times of the desired feature. This is possible by looking at the first values that reach the signal baseline on the left and right side of the peak with the `findBorders` function. From there, wrongly detected vibrations confounded with movements have been eliminated.

Movement detection is far more accurate than vibration detection due to the presence of movement residuals over higher frequencies and intensity of the response.

## 2.3 Summary statistics

Summary statistics include the following formulas:

$$\mu = \frac{1}{n}\sum_{i=1}^{n} x_i \tag{5}$$

Where $\mu$ is the mean, $n$ is the number of samples, and $x_i$ is the sample at the i-th position.

$$\tilde{x} = \frac{1}{2}\left(x_{\left(\frac{n}{2}\right)} + x_{\left(\frac{n}{2}+1\right)}\right) \tag{6}$$

Where $\tilde{x}$ is the median, and $n$ is the number of samples.

$$\sigma = \sqrt{\frac{1}{n}\sum_{i=1}^{n}(x_i - \mu)^2} \tag{7}$$

Where $\sigma$ is the standard deviation, $n$ is the number of samples, $x_i$ is the sample at the i-th position, and $\mu$ is the mean.

# 3 Results

## 3.1 Summary statistics of response box data

A plot of the response times over the iteractions differentiated by test type can be seen in Figure 6. Moreover, the results of the summary statistics for this dataset can be seen in Table 1.

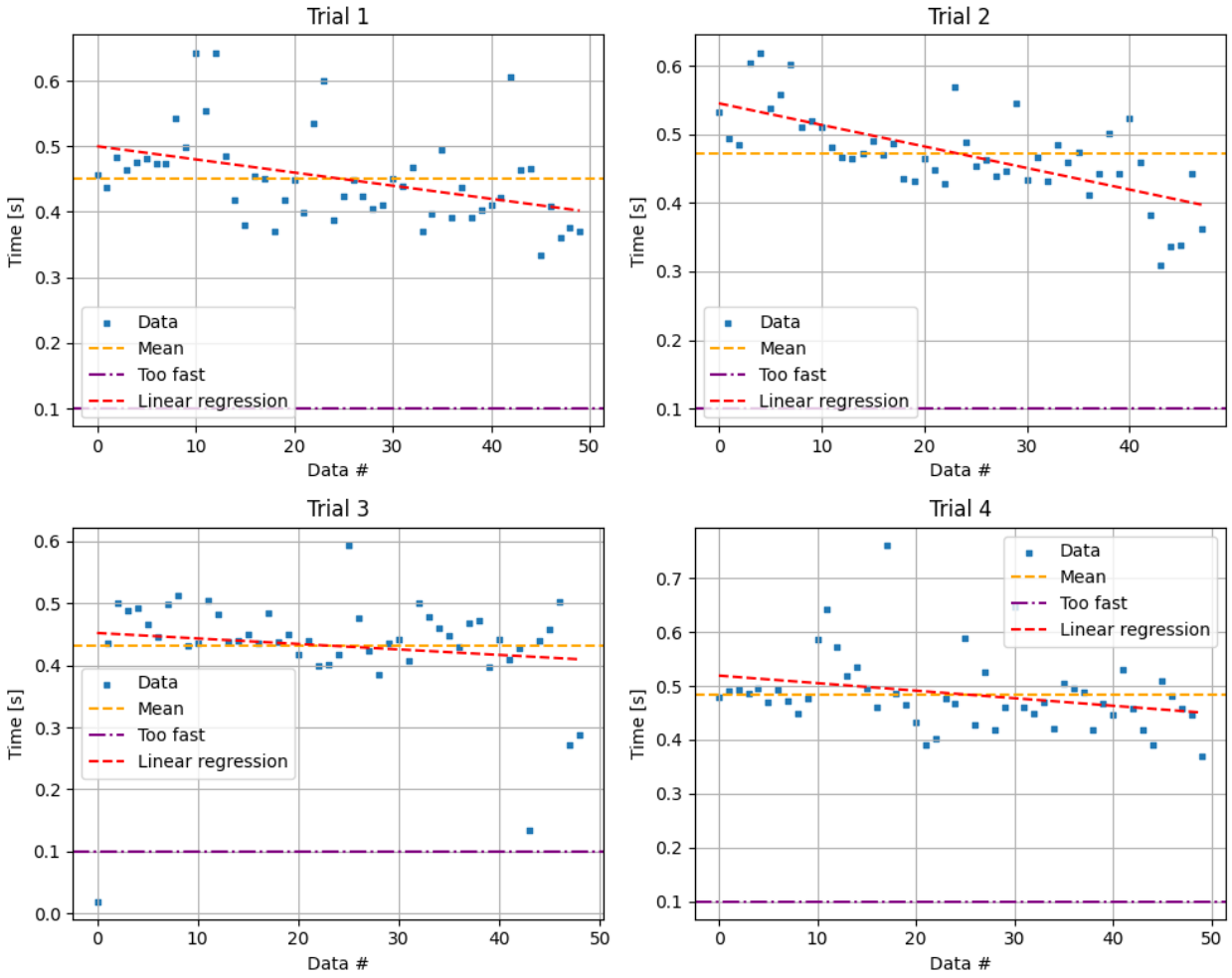


***Figure 6:*** *Plot of response times over each test for each trial*

***Table 1:*** *Unfiltered results*

| Test type | Max $[s]$ | Min $[s]$ | Mean $[s]$ | Median $[s]$ | Standard Deviation $[s]$ |
|---|---|---|---|---|---|
| 1 | 0.643 | 0.333 | 0.451 | 0.444 | 0.069 |
| 2 | 0.620 | 0.310 | 0.472 | 0.467 | 0.064 |
| 3 | 0.593 | 0.020 | 0.431 | 0.440 | 0.089 |
| 4 | 0.761 | 0.370 | 0.485 | 0.473 | 0.069 |

As shown in Table 1, trial 3 yields the fastest response time overall. However, the minimum is not physiologically possible, since it has value $0.02s < 0.1s$. Therefore, is filtered with a threshold at $0.1s$ as shown in Table 2. Nonetheless, trial 3 is still the overall fastest.

***Table 2:*** *Filtered results by eliminating data that is lower than 0.2 and higher than 0.6*

| Test type | Max $[s]$ | Min $[s]$ | Mean $[s]$ | Median $[s]$ | Standard Deviation $[s]$ |
|---|---|---|---|---|---|
| 1 | 0.643 | 0.333 | 0.451 | 0.444 | 0.069 |
| 2 | 0.620 | 0.310 | 0.472 | 0.467 | 0.064 |
| 3 | 0.593 | 0.135 | 0.439 | 0.441 | 0.068 |
| 4 | 0.761 | 0.370 | 0.485 | 0.473 | 0.069 |

Furthermore, the Linear regression entry in the legend from Figure 6 is remarkable: subjects were first familiarized to the task and practiced until they had an average $< 0.5s$ for homotopic responses. Therefore, the first part of the learning curve is not visible in the plots. However, an improvement is still noticeable during the experiment.

By looking more closely at the data shown in Table 2, it is noticeable that the median diverges from the mean by $1$ to $2.4\%$ depending on the presence of outliers (the more the higher). Therefore, it is evident that they are close to each other.

Usually, the choice between mean and median is based on the distribution of the data and the presence of outliers since the median is less affected by the aforementioned. By doing a Shapiro-Wilk test it is noticeable that most of the trials are most likely not normally distributed (Table 3). Therefore, the median is a more appropriate choice compared to the mean to summarize the behavior of the data.

***Table 3:*** *Shapiro-Wilk Test of the filtered data*

| **Trial** | **p-value** | **Outcome** |
|---|---|---|
| 1 | 0.0015 | Not normally distributed. |
| 2 | 0.1536 | May be normally distributed. |
| 3 | $7.4296 \times 10^{-7}$ | Not normally distributed. |
| 4 | $4.6053 \times 10^{-5}$ | Not normally distributed. |

## 3.2 EMG analysis

By analyzing the given EMG and box data, the following conclusion has been reached:

- Type 1 trials correspond to an ADM response.
- Type 2 trials correspond to a FDI response.
- Type 3 trials correspond to a FDI response.
- Type 4 trials correspond to an ADM response.

This has been assessed by checking the box trials against the detected moving finger.

Some trials have not been picked up by the boxes and results in Table 4 shows that the subject responded with the FDI on the trials that the box didn't pick up

| Test number | Test type | Detected response |
|---|---|---|
| 9 | 2 | FDI |
| 27 | 3 | FDI |
| 32 | 2 | FDI |

***Table 4:*** *Results that the boxes didn't pick up*

By comparing the response time from the box and the EMG file, the results from Figure 7 can be seen: there is an almost constant offset of $100ms$ between the EMG response time and the box response time. Furthermore, from the input data is is evincible that the EMG's sampling frequency is $2kHz$.

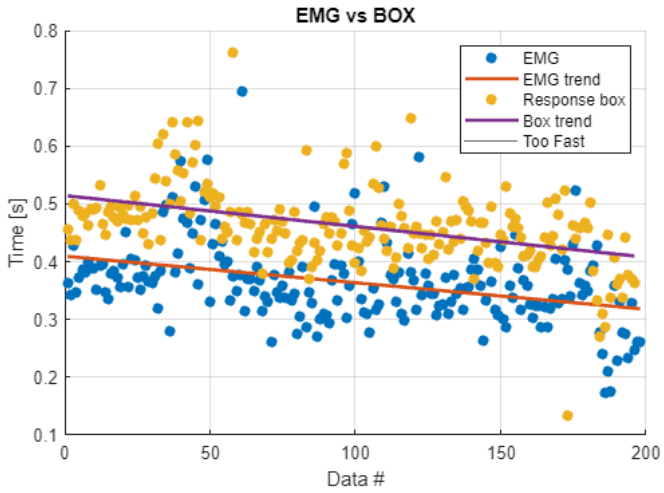


***Figure 7:*** *Plot of the reaction time difference over tests of EMG and Box data.*

By following the same steps as Table 2, Table 5 is obtained. It is evident that the tables show similar trends, with trial 3 being the test with the fastest response time overall. Furthermore, trial 4 has the slowest response times of all.

Test 2 and test 3 imply a FDI response where the slower one (T2) is the heterotopic response, which implies a conflict between the input (vibration and color on the screen) and the output (FDI or ADM). On the other hand, the faster one (T3) represents the homotopic response, where there is no conflict between input and output.

Test 1 and test 4 imply an ADM response where T1 is homotopic and T4 is heterotopic.

In actuality, T1 and T2 are heterotopic, while T3 and T4 are homotopic. Therefore, T1 and T4 don't align with the above logic. This could be due to finger control and sensitivity differences. However, as shown in Figure 6, a more inclined regression slope is noticeable. This implies learning over interactions, leading to adaptation to the conflict task.

It is noticeable that between the homotopic tests, FDI is faster than ADM.

| Test type | Max $[s]$ | Min $[s]$ | Mean $[s]$ | Median $[s]$ | Standard Deviation $[s]$ |
|---|---|---|---|---|---|
| 1 | 0.576 | 0.241 | 0.358 | 0.343 | 0.080 |
| 2 | 0.511 | 0.209 | 0.365 | 0.370 | 0.064 |
| 3 | 0.495 | 0.173 | 0.338 | 0.339 | 0.055 |
| 4 | 0.694 | 0.276 | 0.393 | 0.384 | 0.072 |

***Table 5:*** *EMG response time results by test.*

Successively, as shown in Figure 7, there is an almost constant time difference between the two data that averages at approximately $0.098s$. Physiologically, it makes sense since there is a delay between the neurological signal and the input on the box.

Lastly, an attempt to extract the onset time of the vibration from the EMG data is made to undo the dependency from the response box. It is relatively successful since the accuracy in determining the test type has been around $80\%$ for all trial types as shown in Table 6. Calculation are done as:

$$\text{Accuracy} = \frac{\text{correct guesses}}{\text{total trials for trial type}} \cdot 100 \tag{8}$$

| Test type | Accuracy $[\%]$ |
|---|---|
| 1 | 82 |
| 2 | 80 |
| 3 | 77.08 |
| 4 | 78 |

***Table 6:*** *Accuracy of test type detection in EMG data.*

## 3.3 Accelerometer analysis

The analysis of the accelerometer data has been the most demanding and trickier to analyze due to the missing segmentation of the data and the high dependence on data with a low Signal to Noise Ratio (SNR).

By analyzing the data in similar ways as Section 3.2, it results that the data is sampled at $2000Hz$ with vibration lengths of $200ms$, and each trial occurs in a $2s$ window. With a simple printout, it is noticeable that D2 (FDI) movements correspond to a blue output, while a D5 (ADM) movements correspond to a yellow output.

An accuracy check of the detected vibration and moving finger is done by checking the box data trial type and the results are satisfactory since accuracy was around $80\%$ for all trial types as shown in Table 7. Calculations are made with Equation 8.

| Test type | Accuracy run 1 $[\%]$ | Accuracy run 2 $[\%]$ |
|---|---|---|
| 1 | 82 | 78 |
| 2 | 87 | 81 |
| 3 | 95 | 91 |
| 4 | 78 | 71 |

***Table 7:*** *Accuracy of test type detection in acceleration data for the first and second run of the subject.*

After leaving out incorrect guesses and not valid outputs, the plot in Figure 8 is derived for reaction times.

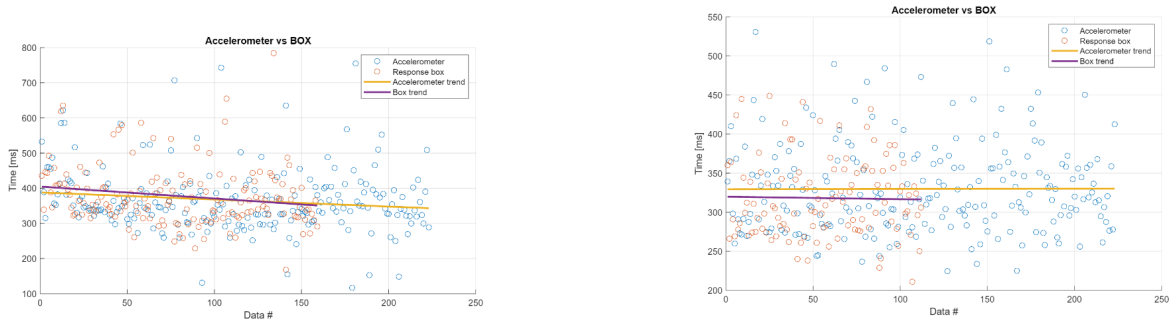


***Figure 8:*** *Accelerometer RT vs box RT. On the left is for the first run and on the right is for the second run.*

As seen in the Figure 8, the linear regression line for accelerometer and box RTs are similar for both runs. However, after estimating the Pearson's correlation coefficient on the data, it was in the order of $10^{-2}$ for both. The result is likely due to imprecision in the detection of RT or, in the best case scenario, due to different indexing of the two datasets. An interesting result is the flattening of the regression curve on the second run. This might be due to adaptation to the task by the subject. Even more interesting is that the accelerometer analysis detects movements even when the response box doesn't as seen by the much bigger sample of data in Figure 8.

Furthermore, summary statistics on RTs are done for both runs as seen in Table 8 for the first, and in Table 9 for the second. The results reinforce the idea that on the second run, the subject adapted to the task leading to a decrease in standard deviation over tests and overall

faster response time. However, it also highlights that there are inaccuracies in the vibration and movement onset and end detection since the means and medians between accelerometer RT and box RT are not always close to each other.

| Test type | Max $[ms]$ | Min $[ms]$ | Mean $[ms]$ | Median $[ms]$ | Standard Deviation $[ms]$ |
|---|---|---|---|---|---|
| 1 | 707 | 148 | 362 | 342 | 86 |
| 2 | 754 | 298 | 389 | 370 | 84 |
| 3 | 622 | 130 | 346 | 344 | 77 |
| 4 | 742 | 259 | 382 | 351 | 102 |
| 1 box | 635 | 260 | 390 | 371 | 94 |
| 2 box | 784 | 291 | 393 | 370 | 89 |
| 3 box | 619 | 229 | 345 | 334 | 69 |
| 4 box | 589 | 168 | 409 | 406 | 89 |

***Table 8:*** *Accelerometer RT results for the first run vs box results.*

| Test type | Max $[ms]$ | Min $[ms]$ | Mean $[ms]$ | Median $[ms]$ | Standard Deviation $[ms]$ |
|---|---|---|---|---|---|
| 1 | 490 | 244 | 346 | 333 | 59 |
| 2 | 434 | 269 | 340 | 346 | 39 |
| 3 | 443 | 225 | 305 | 302 | 49 |
| 4 | 531 | 245 | 343 | 327 | 67 |
| 1 box | 357 | 238 | 277 | 276 | 33 |
| 2 box | 450 | 256 | 342 | 341 | 48 |
| 3 box | 445 | 211 | 307 | 296 | 48 |
| 4 box | 317 | 299 | 308 | 308 | 12 |

***Table 9:*** *Accelerometer RT results for the second run vs box results.*

# 4 Discussion and Conclusion

Overall, the report dives into different methods for analyzing a conflict task by going through EMG data, accelerometer data, and summary statistics.

Results from device data (Table 5-8-9) align with results from box data (Table 2. Therefore, overall an homotopic D2 (FDI) response is the fastest, while an heterotopic D5 (ADM) response is the slowest. Moreover, D5's RT is generally slower than D2's. This might be due to the lower control capability of the user on D5. Furthermore, trial type detection for both EMG and accelerometer data are around $80\%$ (Table 6-7), making it an acceptable automatization. Therefore, results show a delay due to task conflict but it is also dependent on the control the patient has on the finger.

Future improvements include:

- improving feature detection so that RTs will be more accurate.
- removing the dependency on box data to increase the validity of the methods.
- add a Graphical User Interface (GUI) to manually adjust data that are wrongly detected.
- make the script more general to adjust for high SNR cases.

In conclusion, physiologically, results are within reason with a moderate degree of error. The methods can be further refined to increase precision and deal with more scenarios. This is valid, especially for accelerometer analysis, where the onsets and end times do not statistically correlate even though they have the same trend.

All the Matlab and Python code used in the project can be found on Github.

# List of Figures

# List of Tables

# References

[1] C. L. Vaughan, *GaitCD*. Howard Place, Western Cape, South Africa: Kiboho Publishers, 1999. OCLC: 1280899182.

[2] M. F. Bear, B. W. Connors, and M. A. Paradiso, *Neuroscience: exploring the brain*. Philadelphia: Wolters Kluwer, 4. ed ed., 2016.

[3] R. Littman, E. Keha, and E. Kalanthroff, "Task conflict and task control: A mini-review," *Frontiers in Psychology*, vol. 10, 2019.

[4] D. Esposito, J. Centracchio, P. Bifulco, *et al.*, "A smart approach to emg envelope extraction and powerful denoising for human–machine interfaces," *Sci Rep*, vol. 13, p. 7768, 2023.

[5] B. Wang, W. Ke, J. Guang, G. Chen, L. Yin, S. Deng, Q. He, Y. Liu, T. He, R. Zheng, Y. Jiang, X. Zhang, T. Li, G. Luan, H. Lu, M. Zhang, X. Zhang, and Y. Shu, "Firing frequency maxima of fast-spiking neurons in human, monkey, and mouse neocortex," *Front Cell Neurosci*, vol. 10, p. 239, Oct 2016.

[6] C. Carvalho, J. Fernández, A. Del-Ama, F. Oliveira Barroso, and J. Moreno, "Review of electromyography onset detection methods for real-time control of robotic exoskeletons," *J Neuroeng Rehabil*, vol. 20, p. 141, Oct 2023.

[7] R. Khusainov, D. Azzi, I. E. Achumba, and S. D. Bersch, "Real-time human ambulation, activity, and physiological monitoring: taxonomy of issues, techniques, applications, challenges and limitations," *Sensors (Basel)*, vol. 13, no. 10, pp. 12852–12902, 2013.